# AZD2171, a Pan-VEGF Receptor Tyrosine Kinase Inhibitor, Normalizes Tumor Vasculature and Alleviates Edema in Glioblastoma Patients

Published in final edited form as:
*Cancer Cell*. 2007 January ; 11(1): 83–95. doi:10.1016/j.ccr.2006.11.021.

# AZD2171, a Pan-VEGF Receptor Tyrosine Kinase Inhibitor, Normalizes Tumor Vasculature and Alleviates Edema in Glioblastoma Patients

**Tracy T. Batchelor**[1,2,10,*], **A. Gregory Sorensen**[3,6,10], **Emmanuelle di Tomaso**[2,11], **Wei-Ting Zhang**[3,6,11], **Dan G. Duda**[2,11], **Kenneth S. Cohen**[4], **Kevin R. Kozak**[2], **Daniel P. Cahill**[5], **Poe-Jou Chen**[3,6,7], **Mingwang Zhu**[3,6], **Marek Ancukiewicz**[2], **Maciej M. Mrugala**[1], **Scott Plotkin**[1], **Jan Drappatz**[8], **David N. Louis**[5], **Percy Ivy**[9], **David T. Scadden**[4], **Thomas Benner**[3], **Jay S. Loeffler**[2], **Patrick Y. Wen**[8], and **Rakesh K. Jain**[2,*]

[1] Department of Neurology, Massachusetts General Hospital and Harvard Medical School, Boston, MA 02114, USA

[2] Department of Radiation Oncology, Massachusetts General Hospital and Harvard Medical School, Boston, MA 02114, USA

[3] Department of Radiology, Massachusetts General Hospital and Harvard Medical School, Boston, MA 02114, USA

[4] Center for Regenerative Medicine, Massachusetts General Hospital and Harvard Medical School, Boston, MA 02114, USA

[5] Department of Pathology, Massachusetts General Hospital and Harvard Medical School, Boston, MA 02114, USA

[6] MGH-HST A.A. Martinos Center for Biomedical Imaging, Massachusetts General Hospital, and Division of Health Sciences and Technology, Harvard Medical School, Boston, MA 02114, and Massachusetts Institute of Technology, Cambridge, MA 02139, USA

[7] Department of Nuclear Science and Engineering, Massachusetts Institute of Technology, Cambridge, MA 02139, USA

[8] Department of Adult Oncology, Dana-Farber Cancer Institute, and Harvard Medical School, Boston, MA 02115, USA

[9] Cancer Therapy Evaluation Program, National Cancer Institute, Bethesda, MD 20892, USA

## SUMMARY

*Correspondence: tbatchelor@partners.org (T.T.B.), jain@steele.mgh.harvard.edu (R.K.J.).
[10]These authors contributed equally to this work.
[11]These authors contributed equally to this work.

Supplemental Data

Supplemental Data include eight tables, two figures, and a movie and are available at http://www.cancercell.org/cgi/content/full/11/1/83/DC1/.

SIGNIFICANCE

This study identifies the onset and duration of a vascular normalization window created by an antiangiogenic agent in a human tumor. These findings also provide evidence that recurrent glioblastomas remain responsive to antiangiogenic therapy following progression during drug interruption. Moreover, viable CECs, which correlated with tumor progression through treatment, constitute different biomarkers than CPCs, which correlated with tumor relapse after drug interruption. On the other hand, plasma bFGF and SDF1α levels increase with tumor progression, highlighting these angiogenic pathways as potential targets for therapy. Finally, this study demonstrated that AZD2171, a multitargeted tyrosine kinase inhibitor, can alleviate edema, a major cause of morbidity in glioblastoma, and is associated with a steroid-sparing effect in these patients.

Using MRI techniques, we show here that normalization of tumor vessels in recurrent glioblastoma patients by daily administration of AZD2171—an oral tyrosine kinase inhibitor of VEGF receptors—has rapid onset, is prolonged but reversible, and has the significant clinical benefit of alleviating edema. Reversal of normalization began by 28 days, though some features persisted for as long as four months. Basic FGF, SDF1α, and viable circulating endothelial cells (CECs) increased when tumors escaped treatment, and circulating progenitor cells (CPCs) increased when tumors progressed after drug interruption. Our study provides insight into different mechanisms of action of this class of drugs in recurrent glioblastoma patients and suggests that the timing of combination therapy may be critical for optimizing activity against this tumor.

## INTRODUCTION

Tumor vessels are structurally and functionally abnormal. This abnormality impairs effective delivery of therapeutic agents to all regions of tumors, creates an abnormal microenvironment (e.g., hypoxia) that reduces the effectiveness of radiation and chemotherapy, and selects for more malignant cells. Antiangiogenic therapy has the potential to normalize structurally and functionally abnormal tumor vasculature and improve the tumor microenvironment (Jain, 2001, 2005). However, when normalization begins or ends in cancer patients treated with antiangiogenic agents and whether this process is reversible are not known (Jain et al., 2006). The specifics of how vascular normalization directly benefits cancer patients are also unclear. Finally, it is also not known if vascular normalization can be detected with currently available imaging or if it requires emerging new noninvasive technology or blood biomarkers. Answering these questions is critical for optimally combining antiangiogenic therapy with cytotoxic therapies and for customizing treatment for individual patients.

To this end, we designed a National Cancer Institute-sponsored phase II clinical trial of AZD2171 (cediranib, AstraZeneca Pharmaceuticals, UK; Wedge et al., 2005)—a potent oral, pan-VEGF receptor tyrosine kinase inhibitor with activity against PDGF receptors and c-Kit—in glioblastoma patients who had failed conventional therapy. Since serial tumor sampling is not possible in brain tumor patients, we measured relative vessel size and permeability, tumor contrast enhancement, and edema-associated parameters in 16 consecutive patients using a series of MRI protocols. Furthermore, we correlated the temporal changes in these parameters with blood molecular (angiogenic cytokines) and cellular (viable CECs and CPCs) biomarkers of vascular response (trial schema; Figure 1A). Our data show that AZD2171 induced vascular normalization in recurrent glioblastomas within 24 hr, that vascular normalization lasted at least 28 days—ideal for combining with a cycle of concurrent chemotherapy or radiotherapy—and that a direct consequence of vascular normalization is alleviation of vasogenic brain edema. Strikingly, tumor vessels became abnormal following drug “holidays” and “renormalized” after drug resumption. Disease progression during treatment correlated with significant increases in plasma bFGF, SDF1α, and viable CEC concentration. In contrast, tumor progression after drug holidays correlated with increased CPC levels. These data not only identify potential new targets for recurrent glioblastoma treatment, but also show that different circulating cell populations (CECs versus CPCs) have value as independent biomarkers in patients with recurrent glioblastoma treated with AZD2171.

## RESULTS AND DISCUSSION

### The Targets of AZD2171 Are Present in Recurrent Glioblastoma Vessels

To determine if the targets of AZD2171 are present in glioblastoma, we performed immunohistochemistry on archival tumor specimens from our subjects obtained at the time of their original diagnosis. VEGFR2, PDGFRα and PDGFRβ were present on the majority of endothelial cells in all 16 patients, whereas VEGFR1 and VEGFR3 were rarely detectable

(Figure 1B). Although we could not obtain biopsy tissue from these patients at the time of recurrence, it is likely that expression patterns were not dramatically affected by prior radiation and chemotherapy. Indeed, in a separate study of glioblastoma patients in which matched pre- and posttreatment specimens were available, the patterns of expression were similar, with a concordance of 100% for the vascular expression of VEGFR2, PDGFRα, and PDGFRβ (overall level of concordance for all AZD2171 targets: 76%) between newly diagnosed and recurrent tumor specimens (Tables S1 and S2 [see the Supplemental Data available with this article online]). Collectively, these data suggest that VEGFR2, PDGFRα, and PDGFRβ—targets for agents such as AZD2171—are present in recurrent glioblastoma.

## Recurrent Glioblastomas Respond to AZD2171 Treatment

Since AZD2171's targets are consistently present on the endothelium in glioblastoma, and the half-life of AZD2171 (12.5–35.4 hr) allows their continuous inhibition with daily administration, we anticipated this agent would be a potent antivascular and normalizing agent. Indeed, all patients showed decreased tumor contrast enhancement (using gadolinium as a tracer) after a single dose of AZD2171 despite an aggressive growth rate of approximately 1% in tumor enhancement volume per day prior to treatment initiation (Figure S1 and Tables S3 and S4). Using volumetric evaluation methods (Sorensen et al., 2001), we detected a decrease in tumor enhancement of more than 50% in 9/16 patients and 25%–50% in 3/16 patients (Figures 2–4 and 5A, and Table S5). Toxicity was modest, and median progression-free survival in this small cohort of patients was 111 days, which compares favorably to that reported from an historical database (Wong et al., 1999) (Figure 6). Similar to other antiangiogenic therapies that target only tumor endothelium, monotherapy with AZD2171 may not improve overall survival, suggesting the need to combine cytotoxic therapies with AZD2171 (median overall survival in our 16 patients was 211 days, compared to a median overall survival of 175 days from an historical database [Wong et al., 1999]).

Despite detection of the targets of AZD2171 in the glioblastoma vasculature in all of our patients, there was considerable variability in tumor responses (Figures 2–5, and Tables S3 and S4). Thus, identification of biomarkers associated with tumor regression is a high priority. The radiographic regressions observed in our study but apparent lack of survival prolongation emphasizes the need for combination studies with AZD2171. It also suggests that the traditional endpoint of tumor enhancement volume may not be the optimal assessment of treatment response. Establishing the optimal timing of antiangiogenic therapies such as AZD2171 in relation to other cytotoxic therapies is a critical challenge (Brown et al., 2004; Grossman and Batara, 2004; Jain et al., 2006; Prados et al., 2006; Reardon et al., 2005; Tremont-Lukats and Gilbert, 2003).

## AZD2171 Induces a Rapid Structural Normalization of Tumor Vessels

In preclinical studies, fractionated radiation or chemotherapeutics are most effective when given during a window of normalization created by antiangiogenic agents (Ansiaux et al., 2005; Segers et al., 2006; Winkler et al., 2004). In a clinical trial in rectal carcinoma patients, a single administration of bevacizumab—a VEGF-specific antibody with a half-life of 2–3 weeks—has been shown to prune approximately half of the tumor vessels and normalize the remaining vasculature by day 12 (Willett et al., 2004, 2005). Key challenges now are to identify the beginning and end of this process and to determine the impact of normalization on the tumor. In murine models, VEGFR2- and VEGF-blockade or downregulation begin to normalize the tumor vasculature by day 1 or 2, as detected by a significant decrease in their mean vessel diameter and permeability (Jain et al., 1998; Kadambi et al., 2001; Tong et al., 2004; Winkler et al., 2004; Yuan et al., 1996). Unlike vascular permeability, tumor vessel size during antiangiogenic therapy has never been reported in cancer patients.

The MRI methods (Dennie et al., 1998; Schmainda et al., 2004) used here demonstrate that in most patients, similar to mouse models, relative tumor vessel size significantly decreased as early as 1 day after the onset of AZD2171 treatment ($p < 0.05$), and it remained decreased at day 28. At day 56, the relative vessel size reverses toward abnormal values ($p < 0.05$ versus day 28 values) in the majority of patients, suggesting the beginning of the closure of the structural vascular normalization window (Figures 3, 4, and 5A, and Figure S2 and Table S3). Our MRI method separately measures blood volume in large and small vessels, where small means a peak sensitivity to vessels 5–10 microns in diameter, and large means all vessels weighted equally. AZD2171 has a more pronounced effect on large microvessels compared to small microvessels, with an immediate decrease in blood volume in large vessels, and decreased blood flow in both small and large vessels (Table S3). These results demonstrate a direct effect of AZD2171 on tumor vasculature, which may be due to vessel pruning and remodeling and/or blockade of angiogenesis.

## AZD2171 Induces a Rapid Onset of Functional Vascular Normalization

VEGF is a potent vascular permeability factor (Dvorak, 2002; Senger et al., 1983). Similar to previous preclinical and clinical studies, we found a significant reduction in vascular permeability (as measured by the transfer constant $K^{trans}$ of contrast agent between plasma and the extravascular extracellular space) (Jackson et al., 2003; Pope et al., 2006; J. Drevs et al., 2005, J. Clin. Oncol., abstract) at days 1 and 28 ($p < 0.01$). Unlike the increase in vessel size, vascular permeability to gadolinium remained decreased through day 112, indicating that this feature of vascular normalization extended beyond 56 days (Figures 2C and 5A, and Table S3). This uncoupling between vessel size and permeability during AZD2171 therapy was not observed in preclinical studies of therapies that exclusively target the VEGF pathway in glioblastoma (Winkler et al., 2004) and may be a consequence of the broader inhibitory spectrum of AZD2171.

Formally, $K^{trans}$ is not solely permeability dependent; it represents a function of both permeability and vessel surface area. Consequently, the significant drop in $K^{trans}$ could be due, in part, to reduced vascular surface area if vessels are shrinking. However, with uncoupling, and a rebound in vessel size, the persistent decrease in $K^{trans}$ indicates that permeability remains reduced. We observed a correlation between uncoupling and elevation of bFGF and SDF1α levels (see below), suggesting that these cytokines may be involved in this process. Although c-Kit expression was not commonly detected in glioblastoma tumor cells or vessels, a systemic effect cannot be excluded, as c-Kit is present and functional in CPCs (Rafii et al., 2002). Also, PDGF receptors were expressed along with VEGFR2 on the endothelial cells of all glioblastomas examined (Figure 1B). However, the effects of PDGFRβ signaling blockade by AZD2171 in endothelial and perivascular cells remain to be elucidated. Similarly, it would be of great interest to establish any direct effect of AZD2171 on glioblastoma cells and, in particular, on the cancer stem cells (Fomchenko and Holland, 2006), which may be responsible for tumor relapse.

## Vascular Normalization by AZD2171 Alleviates Vasogenic Edema

A direct consequence of the vascular abnormalities in glioblastoma is vasogenic brain edema, which is a significant cause of morbidity in these patients. The most widely used and effective therapy for vasogenic edema is corticosteroid administration. However, corticosteroid-related complications are frequent and detrimental for glioblastoma patients. Preclinical studies have demonstrated that VEGF blockade can reduce edema due to ischemic injury (Weis and Cheresh, 2005). Whether VEGF blockade could reduce vasogenic edema in brain tumor patients has not been quantitatively assessed. Therefore, we used three different MRI techniques to assess and quantify vasogenic brain edema in our study: (1) T2-weighted fluid-attenuated inversion recovery (FLAIR) lesion volumes; (2) trace apparent diffusion coefficient

of water (ADC); and (3) extracellular extravascular space fraction ($v_e$). (Figures 2–4, and Figure S2 and Table S3). All these measurements demonstrated rapid and significant reduction in vasogenic edema for the duration of AZD2171 therapy ($p < 0.01$; Figure 5B). Consequently, 14 of 15 patients with mass effect (e.g., displacement of ventricles, midline shift) due to their recurrent tumor showed reduction in the mass effect and improvement in the visibility of white matter fiber anatomy (Figures 2–4, and Movie S1).

Steroid usage was reduced in these subjects compared to typical recurrent glioblastoma patients. Five patients did not require steroids, and of the 11 patients who received corticosteroids during the course of AZD2171 therapy, 8 had their dose reduced and 3 had corticosteroids discontinued. All patients who progressed on this study required corticosteroids after discontinuation of AZD2171. These data demonstrate that AZD2171—and the resulting vascular normalization—efficiently decreases edema in glioblastoma patients and is associated with a steroid-sparing effect in this population. Corticosteroids are not only associated with detrimental side effects in cancer patients but may also diminish the effectiveness of chemotherapy. Dexamethasone has been shown in vitro to reduce the efficacy of concurrently administered chemotherapy (Das et al., 2004). The antiedema effects of AZD2171 may improve neurological function and allow better clinical tolerance of fractionated radiation, since well-known adverse effects of radiation are brain/tumor necrosis and exacerbation of vasogenic edema with increased intracranial pressure. There is anecdotal evidence that standard chemoradiation (temozolomide and fractionated radiation) may increase the risk of tumor necrosis and brain edema (Chamberlain et al., 2006). Thus, for multiple reasons the combination of AZD2171 with chemoradiation in newly diagnosed glioblastoma patients is worthy of investigation.

## Vascular Normalization by AZD2171 Is Reversible

Since some patients required drug interruption due to toxicity (referred to as a drug holiday; see Table S6), we used this opportunity to gain further mechanistic insight into vessel normalization. Radiographic analyses provided evidence that drug holidays were associated with an increase in the CE-T1 volume (Figure 7A); of note, drug holidays within 14 days of a scheduled MRI were associated not only with a significant increase in the enhancement volume, but also in extracellular-extravascular volume fraction ($v_e$, $p < 0.05$; Table S7). Two of these five patients (patients 4 and 10) underwent MRI studies before, during, and after a drug holiday. In these two patients, the enhancement volume and permeability were smaller than baseline prior to the holiday, increased substantially during the holiday, and then regressed again after the holiday when AZD2171 was resumed (Figure 7B). These data reveal the reversibility of AZD2171-induced vascular normalization and the plasticity of human tumor vessels.

## Circulating Biomarkers Correlate Differentially with Tumor Response to AZD2171 Treatment

A major challenge in using antiangiogenic agents remains identification and validation of molecular and cellular biomarkers of response. Currently, no such parameters have been discovered for bevacizumab (Ince et al., 2005; Jubb et al., 2006). We examined molecular (angiogenic cytokines and soluble receptors) and cellular (viable CECs and CPCs) markers in patients who progressed while on AZD2171 and in those who had drug holidays, and we found significant changes. Consistent with previous reports on the effects of anti-VEGF agents (Motzer et al., 2006; Willett et al., 2005; J. Drevs et al., 2005, J. Clin. Oncol., abstract), our blood biomarker analyses showed significant increases in VEGF and PlGF and decreases in sVEGFR2 plasma levels throughout AZD2171 treatment (Table S8). In patients who experienced tumor progression while on AZD2171, increases in tumor enhancement volume were associated not only with decreases in levels of PlGF and increases in sVEGFR2 in plasma, but also with significant increases in plasma levels of bFGF and SDF1α ($p < 0.05$; Table 1). Moreover, there was a statistically significant ($p < 0.05$; Table 1) positive correlation between

both bFGF and SDF1α levels and vessel size measured by MRI. It has been previously reported that bFGF (a potent mitogen for endothelial cells) can compensate for VEGF and induce angiogenesis in transplanted tumors (Yoshiji et al., 1997). These findings were also confirmed recently in oncogene-induced insulinomas (Casanovas et al., 2005). However, the clinical evidence for this compensation has been lacking. In addition, preclinical and clinical evidence has supported a critical role for SDF1α in glioblastoma neovascularization (Aghi et al., 2006; Rempel et al., 2000). Our work provides clinical evidence that bFGF and SDF1α may play a role in glioblastoma relapse in patients treated with anti-VEGF agents. Based on these findings, we suggest that bFGF and SDF1α should be considered as biomarkers as well as potential targets for extending the normalization window.

Viable CECs and CPCs have been previously proposed as biomarkers for antiangiogenic therapy, but a clear consensus on the surface markers used to identify these blood-circulating cells is currently lacking (Bertolini et al., 2006; Duda et al., 2006). Subsets of CPCs (e.g., endothelial and/or hematopoietic progenitors) have been suggested to play an important role in angiogenesis (Rafii et al., 2002; Stoll et al., 2003), and moreover, these cells may represent targets for antiangiogenic therapy (Carmeliet, 2005). Indeed, we have found that bevacizumab decreases the number of viable CECs and CPCs in rectal carcinoma patients (Willett et al., 2004, 2005). But whether viable CECs and CPCs are biomarkers of response to, or progression through, antiangiogenic therapy in patients is unclear. In addition, whether viable CECs play any role in tumor neovascularization or during antiangiogenic therapy is not currently known. In this study, we found that viable CEC number increased significantly with tumor enhancement volume measured by MRI at four time points (days 1, 28, 56, and 112) during AZD2171 therapy ($p < 0.05$; Table 1). In addition, viable CEC levels were higher in the patients who experienced disease progression during AZD2171 therapy ($n = 11$) compared to patients without progression at day 112 ($n = 5$; median peak values 1.58 and 0.95, respectively, evaluated at all eight time points before and after AZD2171 treatment, $p < 0.05$). No such correlation was seen for CPCs.

After drug holidays VEGF and PlGF plasma levels decreased significantly ($p < 0.01$; Table 1). Interestingly, blood biomarker analyses after drug holidays also showed that glioblastoma progression (as measured by MRI) after the interruption of AZD2171 therapy correlated with significant increases in the number of CPCs ($p < 0.01$) and with a trend toward increased plasma bFGF (Table 1). These findings suggest a differential role for CPCs versus viable CECs in the assessment of clinical outcomes in recurrent glioblastoma. These data also emphasize the critical importance of using multiple viability and cell surface markers to identify these distinct populations and differentiate them from other blood circulating cells, such as non-viable CECs (likely shed by the tumor endothelium during therapy) or mature hematopoietic cells (Duda et al., 2007). In contrast, bFGF and SDF1α appear to be more generic biomarkers of glioblastoma relapse. Of interest, the expression of AZD2171's targets (VEGF and PDGF receptors or c-Kit) on tumor cells from the initial biopsy specimen did not correlate with response in these recurrent glioblastoma patients.

## Conclusion

In summary, we report an immediate and significant normalizing effect of AZD2171 in 16 patients with recurrent glioblastoma—indicative of a direct effect on tumor vasculature—with promising tumor responses and biomarker correlations. The sustained reduction in permeability is associated with a reduction in tumor-associated vasogenic brain edema and clinical benefit in most patients as measured by avoidance or reduction of corticosteroids. The antiedema effects of AZD2171 observed in our study raise the possibility that anti-VEGF therapies might prove beneficial for vasogenic brain edema secondary to primary and metastatic brain tumors or other neurological diseases. Other features of vascular normalization

(e.g., decreased blood vessel size) were maintained for at least 28 days, which suggests that administration of AZD2171—or potentially other VEGF inhibitors—with concurrent cytotoxic therapies *from the onset* may be particularly beneficial within this window of opportunity. Since AZD2171 monotherapy may not increase survival, future trials of AZD2171 with or without chemotherapy are planned to validate these findings and test these hypotheses.

## EXPERIMENTAL PROCEDURES

### Study Design

The current phase 2 investigational study was approved by the Institutional Review Board at the Dana-Farber/Harvard Cancer Center. Inclusion criteria for this study were the following: pathological diagnosis of glioblastoma; imaging or pathological evidence of recurrent glioblastoma; ability to provide informed consent; Mini-Mental Status Examination (MMSE) score ≥ 15; age ≥ 18; adequate functional status (Karnofsky Performance Score ≥60); elapse of 3 months since prior radiation, 3 weeks since prior non-nitrosourea-based chemotherapy or 6 weeks since prior nitrosourea-based chemotherapy; treatment with no more than two prior chemotherapy regimens; stable dose of corticosteroids for at least 5 days prior to the first study MRI scan; adequate bone marrow (absolute neutrophil count ≥ 1500/μl; platelet count ≥ 100,000/μl; hemoglobin ≥ 8 g/dl); creatinine within normal institutional limits or creatinine clearance ≥ 60 ml/min/1.73 $m^2$ for patients with creatinine greater than normal institutional limits. Exclusion criteria for this study included the following: major surgery (including craniotomy for tumor resection or biopsy) within 4 weeks; concurrent use of anticoagulant drugs or antiplatelet drugs; mean corrected QT interval > 470 milliseconds or patients with familial prolonged QT syndrome; ≥1+ proteinuria on two successive urine dipstick assessments; pregnant women; patients with uncontrolled hypertension or other serious medical illnesses (including but not limited to unstable angina, cardiac arrhythmia, active infection, symptomatic congestive heart failure); patients infected with the human immunodeficiency virus; concurrent use of enzyme-inducing antiepileptic drugs; imaging (CT or MRI) evidence of intratumoral or peritumoral hemorrhage deemed significant by the treating physician; patients with a history of coagulopathy. All patients were provided blood pressure monitoring devices for use at home. Blood pressure diaries were recorded for all patients. In patients who developed hypertension, a standard algorithm for management was followed. The accrual goal for this trial of 31 patients has been achieved. It is not placebo controlled.

We are reporting results on the first 16 consecutive patients accrued; no selection criteria were employed to include patients in this analysis (for further details, see http://clinicaltrials.gov, identifier NCT00254943).

Eligible patients received AZD2171 (cediranib, AstraZeneca Pharmaceuticals, Cheshire, UK) at a dose of 45 mg daily by mouth continuously. There was no maximal length of therapy. Dose-limiting toxicities were defined as any grade 3 nonhematological or grade 4 hematological toxicities. In patients experiencing dose-limiting toxicities, AZD2171 could be reduced to 30 mg (dose reduction 1), 20 mg (dose reduction 2), or 10 mg (dose reduction 3). Patients could also reduce or terminate administration in consultation with their neurooncologist for any other side effect considered to be related to AZD2171.

Patients were followed by serial neurological and physical examinations every 28 days; dynamic contrast enhanced MRI; diffusion tensor MRI; perfusion weighted MRI on days −5 (plus or minus 2 days) −1, +1 (at least 24 hr after the first administration of the AZD2171 and before the second dose), +26–28, +54–56, and standard contrast-enhanced cranial MRI at baseline and every 60 days thereafter. In addition patients' blood (30 ml) was collected on days −1, 0, +2, +10, +28, and once every 28 days thereafter for the following assays: circulating

endothelial cells, circulating progenitor cells, and plasma levels of VEGF-A, sVEGFR1 and -2, PlGF, SDF1α, bFGF, and interleukin-8 (see below).

All patients were treated until there was radiographic or clinical evidence of disease progression. Patients could withdraw from the study at any time.

The primary endpoint of this phase 2 study was to determine the proportion of patients alive and progression-free at 6 months (APF6). Secondary endpoints include radiographic responses, toxicity, overall survival, as well as biological and imaging endpoints.

## MRI Methodology

**Image Acquisition—**Each patient underwent scanning on the same 3 Tesla MRI system (TimTrio, Siemens Medical Solutions, Malvern, PA). All patients were scanned at two baseline time points, typically 3 to 7 days (average: 5.7) and then 1 day before the first treatment, as well as 1 day and 28 days after the first treatment. (There were two deviations from this: patients 2 and 11 had the second baseline scan at 2 days before the first treatment.) Thirteen of 16 patients were also scanned about 56 days after the first treatment, and 5 of the 16 patients (who had not experienced progression) were scanned about 112 days after the first treatment. Each scanning session consisted of the following sequences:

1. Scout. The "AutoAlign" method of producing scout images was used to improve scan-to-scan reproducibility. Briefly, this method acquires two low-resolution whole-head scans (2.5 mm isotropic voxels) at different flip angles within 46 s, and uses a computer algorithm to compare the current location of the head with a predefined atlas. This localization is then used to ensure that the slice prescriptions are identical between scan sessions, even across many months (Benner et al., 2006; van der Kouwe et al., 2005). Imaging time: 46 s.
2. T2-weighted images. A single-slab, three-dimensional, T2-weighted turbo-spin-echo sequence with high sampling efficiency ("SPACE") (Lichy et al., 2005) was used at high resolution. Specific imaging parameters: 0.9 mm isotropic, 192 slices, 256 × 256 matrix, 24 cm FOV, TR 3200 ms, effective TE 494 ms. Imaging time: 4:30 (minutes:seconds).
3. FLAIR images. Axial fluid-attenuated inversion recovery images were acquired with TR 10,000 ms, TE 70 ms, and 5 mm slice thickness, 1 mm interslice gap, and 0.6 mm × 0.45 mm in-plane resolution; 23 slices, 384 × 512 matrix. Imaging time: 3:02.
4. T1 images. Axial images were obtained prior to the injection of contrast. TR 600 ms, TE 12 ms, 5 mm slice thickness, 1 mm interslice gap, 0.45 mm in-plane resolution; 23 slices, 384 × 512 matrix. Imaging time: 1:59.
5. Dynamic contrast-enhanced images. This is a series of acquisitions of a 50.6 mm thick slab consisting of 20 slices. All scans are 2.9 mm × 2.0 mm in-plane resolution, with a 2.1 mm slice thickness, 0.4 mm interslice gap, using a fast gradient echo technique (TR 5.7 ms, TE 2.73 ms). Data to allow computation of a T1 map of the tissue of interest are initially created using five different flip angles (2°, 5°, 10°, 15°, 30°). Then, the same slab of tissue is sampled with a 10° flip angle every 5.04 s for 252 s (50 time points), and 0.1 mMol/kg of Gd-DTPA was injected 52 s after the beginning of the acquisition at 5 cc/s. Imaging time: 4:12.
6. Diffusion-weighted imaging. 60 slices of twice-refocused echo-planar diffusion-weighted images were acquired with TR 7500 ms, TE 84 ms, and a b-value of 700 s/mm$^2$ in 42 directions as well as 7 low b-value images (b ~0 s/mm$^2$) to allow

reconstruction of the diffusion tensor at each voxel. Resolution was 2 mm isotropic, with a 128 × 128 matrix. Imaging time: 6:30.

7. Dynamic susceptibility contrast imaging. A 75 mm slab of tissue was imaged using a dual-echo, combined gradient-echo, and spin-echo echo planar sequence to enable relative vessel size mapping (Dennie et al., 1998; Pathak et al., 2001; Schmainda et al., 2004). This sequence acquires two images after each 90° RF excitation: a gradient echo image (TE 34) and a spin echo image (TE 103); each image had 1.7 mm in-plane resolution and 5 mm through-plane resolution (128 × 128 matrix). There was a 2.5 mm interslice gap and 10 slices. 120 blocks of images were acquired, with a block acquired every 1.33 s. 0.2 mmol/kg of Gd-DTPA was injected at 5 cc/s after 85 s of imaging. Imaging time: 2:45.

8. Postcontrast T1-weighted imaging. Axial T1-weighted images were acquired exactly as precontrast, as described above. In addition, a 3D magnetization prepared rapid gradient echo (MP-RAGE) volumetric acquisition was performed, with 1 mm isotropic voxels, TR 2530, TE 3.5 ms, 256 × 256 matrix, 176 slices. Imaging time: 6:06.

## Image Analysis

**Volumetrics—**Enhancing lesions and areas of T2 abnormality on FLAIR images were quantitatively analyzed by an experienced neuroradiologist blinded to the order of the scans and treatment status of the patients. The lesions were outlined using a volumetric approach described previously (Sorensen et al., 2001) that includes outlining each enhancing voxel on postcontrast scans and then summing the voxels to calculate an overall lesion volume.

**Map Synthesis: Blood Volume, Blood Flow, and Relative Vessel Size Maps—**Relative cerebral blood volume of larger vessels (gradient echo images) and smaller vessels (spin echo images) as well as cerebral blood flow were calculated using a standard deconvolution technique (Ostergaard et al., 1996), with blood volume corrected for leakage of the contrast agent across the blood-brain barrier (Boxerman et al., 2006; Law et al., 2002). These maps are relative and therefore unitless. Relative vessel size maps were created using the ratio of delta-R2* to delta-R2, according to published approaches (Dennie et al., 1998; Pathak et al., 2001; Schmainda et al., 2004). This provides a voxel-by-voxel estimate of the relative radius of the microvasculature, with larger vessel diameter corresponding to brighter signal.

**Apparent Diffusion Coefficient Maps—**Maps of apparent diffusion coefficient (ADC) (Oh et al., 2005) were created from the low and high b-value images using custom-written software implementing the standard Steskjal-Tanner diffusion approximation. This provides an estimate of the relative water self-diffusion or water mobility on a voxel-by-voxel basis; higher values represent a greater degree of water mobility, and the units of these maps are in area/time, typically $mm^2/s$.

**Permeability Maps—**Dynamic contrast-enhanced MRI data were processed using custom-made software written in Matlab (The MathWorks, Natick, MA), following standard published approaches, including maps of $K^{trans}$ (corresponding roughly to wash-in rates of the contrast agent) (Tofts et al., 1999) and $v_e$ (extracellular-extravascular volume fraction). These references provide highly detailed descriptions of these parameters and their biophysical meaning. $K^{trans}$ does not fully correspond to permeability in each regime, but it is related to the permeability-surface area product of the capillary bed in non-flow-limited situations.

**Synthetic Map Analysis—**The outlines generated in the volumetric analysis of the second baseline (day −1) were coregistered to the synthesized maps (CBV, CBF, vessel size, $K^{trans}$, ADC) and median values across the entire enhancing lesion (for CBV, CBF, vessel size, and $K^{trans}$) or entire FLAIR lesion abnormality (for ADC) were computed. As all of the values other than ADC were considered relative rather than absolute, maps were normalized to each other using an unaffected area of gray and white matter typically located distantly, such as in the contralateral hemisphere.

## Immunohistochemical Analyses in Tissue Specimens

Archival tissues had to be available for patients to enroll in the clinical trial. Five micron thick paraffin sections were obtained for the 16 patients. Immunostaining was performed using standard heat antigen retrieval in citrate buffer unless otherwise specified by the antibody manufacturer. Detection of the primary antibody was done using the HRP visualization system from Dako EnVision in combination with DAB and counterstained with Hematoxilin. The primary antibodies were as follows: CD31 (DAKO N1596) prediluted antibody; α-SMA (DAKO M0581) 1:5000; VEGFR1 (R&D Mab321) 7.5 μg/ml; VEGFR2 (Cell Signaling 2479) 1:125; PDGFRα (Cell Signaling 3164) 1:50; PDGFRβ (Cell Signaling 3169) 1:50.

A subset of seven patients diagnosed with recurrent glioblastoma (diagnosis confirmed by Dr. D. Louis, neuropathologist) for whom tissue specimens were available from both the initial diagnostic procedure and from a pathologically confirmed recurrence were identified from the Massachusetts General Hospital Neuropathology database. Sections from the identified specimen were labeled as described above and used to determine retention of a given molecular target at the time of recurrence.

## Measurement of Angiogenic Proteins in Plasma

Peripheral blood was obtained with informed consent from patients with recurrent glioblastoma enrolled in a phase 2 trial of AZD2171 at base line, 8 hr, 2 days, 9 days, and 28 days following the first dose of AZD2171 and every 28 days thereafter. Blood was collected in an EDTA-containing vacutainer, spun down, and plasma was aliquoted, and frozen immediately. Plasma analysis was carried out for circulating VEGF, PlGF, soluble VEGFR1, and bFGF using multiplex ELISA plates from Meso-Scale Discovery (Gaithersburg, MD) as well as soluble VEGFR2, SDF1-α, and IL-8 from R&D System (Minneapolis, MN). Every sample was run in duplicate.

## Circulating Cell Evaluation by Flow Cytometry

Blood circulating cells were phenotyped and enumerated by flow cytometric analyses of CD31, CD34, CD45, and CD133 expression using fluorescence-labeled monoclonal antibodies and a standard protocol in fresh samples (Duda et al., 2006, 2007). Fluorescence-labeled isotype-matched nonspecific immunoglobulin G (IgG) antibodies were used as controls. Flow cytometry was performed on FACSVantage instruments (Becton Dickinson, San Jose, CA), as described. Cell concentrations were calculated as percentages of the total number of mononuclear cells after an evaluation of at least 100,000 cellular events. The quantitative analysis end point was the change in the fraction of $CD31^{bright}CD34^{+}CD45^{-}$ and $CD133^{+}CD34^{+}$ cells within the mononuclear blood cell population in patients receiving AZD2171 treatment (see below). Percent values were obtained at day −1, before initiation of the therapy, and then at 8 hr and 2, 9, 28, and 56 days after the first ingestion of the drug. Posttreatment values were compared with pretreatment values in individual patients using the Wilcoxon signed rank test.

### Statistical Analysis

Statistical comparisons between MRI parameters, protein levels, and cell counts measured on different study days were performed with a two-tailed paired exact Wilcoxon test (Hollander and Wolfe, 1973) except for Table S3, where we used a two-tailed, exact binomial test. The effect of drug holidays on these variables (after log-transformation) was tested in a mixed effects model (Demidenko, 2004) where random effect part included a patient-specific intercept and fixed effect part included a nonlinear function of time from beginning of the study (B-spline with three knots) and a dummy variable indicating the history of drug holidays. It was assumed that the effect of transient drug holidays lasted up to 2 weeks after resuming the use of study drug; we conducted sensitivity analysis with different values of this parameter (4 week duration and indefinite duration). The effect of tumor response on log-transformed cytokine levels or circulating cell levels was tested in a similar mixed effects model including patient-specific intercept and a fixed effects part consisting of a B-spline function of time and the percentage of tumor volume with respect to baseline measurement. Finally, the effect of log-transformed MRI parameters and protein levels on vessel size was tested in a mixed linear model including patient-specific intercept, vessel size at baseline, and a B-spline function of time. Peak levels of circulating cells were compared by an exact Wilcoxon test.

## Supplementary Material

Refer to Web version on PubMed Central for supplementary material.

## Acknowledgments

The authors thank H. Chen for thoughtful comments and suggestions on this manuscript; R. Tong for his help in the planning of this trial; K. David, L. Doherty, M. Foley, D. Gigas, R. Klein, J. Kracher, A. Lee, A. Newcomer, L. Ostrowsky, S. Roberge, C. Smith, P. Yeo, and J. Zimmerman for technical support; W. Copen, A. Guimaraes, A. Singhal, O. Wu, and R. Wang for assistance with image acquisition and analysis. This work was supported by an NIH Grant (R21CA117079 to T.T.B.); partial support was obtained from: NIH grants P41-RR14075, M01-RR-01066, P01CA80124, R01CA115767, and R01CA57683; the Richard and Nancy Simches Endowment for Brain Tumor Research; the Montesi Family Fund; MIND Institute; and an AACR-Genentech BioOncology Career Development Award. R.K.J. is a consultant and grantee of AstraZeneca Pharmaceuticals and has received honoraria for presentations at Roche and Pfizer-sponsored symposia.

## References

Aghi M, Cohen KS, Klein RJ, Scadden DT, Chiocca EA. Tumor stromal-derived factor-1 recruits vascular progenitors to mitotic neovasculature, where microenvironment influences their differentiated phenotypes. Cancer Res 2006;66:9054–9064. [PubMed: 16982747]

Ansiaux R, Baudelet C, Jordan BF, Beghein N, Sonveaux P, DeWever J, Martinive P, Gregoire V, Feron O, Gallez B. Thalidomide radiosensitizes tumors through early changes in the tumor microenvironment. Clin Cancer Res 2005;11:743–750. [PubMed: 15701864]

Benner T, Wisco JJ, van der Kouwe AJ, Fischl B, Vangel MG, Hochberg FH, Sorensen AG. Comparison of manual and automatic section positioning of brain MR images. Radiology 2006;239:246–254. [PubMed: 16507753]

Bertolini F, Shaked Y, Mancuso P, Kerbel RS. The multifaceted circulating endothelial cell in cancer: towards marker and target identification. Nat Rev Cancer 2006;6:835–845. [PubMed: 17036040]

Boxerman JL, Schmainda KM, Weisskoff RM. Relative cerebral blood volume maps corrected for contrast agent extravasation significantly correlate with glioma tumor grade, whereas uncorrected maps do not. AJNR Am J Neuroradiol 2006;27:859–867. [PubMed: 16611779]

Brown CK, Khodarev NN, Yu J, Moo-Young T, Labay E, Darga TE, Posner MC, Weichselbaum RR, Mauceri HJ. Glioblastoma cells block radiation-induced programmed cell death of endothelial cells. FEBS Lett 2004;565:167–170. [PubMed: 15135073]

Carmeliet P. Angiogenesis in life, disease and medicine. Nature 2005;438:932–936. [PubMed: 16355210]

Casanovas O, Hicklin DJ, Bergers G, Hanahan D. Drug resistance by evasion of antiangiogenic targeting of VEGF signaling in late-stage pancreatic islet tumors. Cancer Cell 2005;8:299–309. [PubMed: 16226705]

Chamberlain MC, Glantz MJ, Chalmers L, Van Horn A, Sloan AE, Lee H. Early necrosis following concurrent temozolomide and radiotherapy in adult patients with glioblastoma. J Clin Oncol Suppl 2006;24(Suppl):1513.

Das A, Banik NL, Patel SJ, Ray SK. Dexamethasone protected human glioblastoma U87MG cells from temozolomide induced apoptosis by maintaining Bax:Bcl-2 ratio and preventing proteolytic activities. Mol Cancer 2004;3:36. [PubMed: 15588281]

Demidenko, M. Theory and Application. New York: John Wiley & Sons; 2004. Mixed Effects Models.

Dennie J, Mandeville JB, Boxerman JL, Packard SD, Rosen BR, Weisskoff RM. NMR imaging of changes in vascular morphology due to tumor angiogenesis. Magn Reson Med 1998;40:793–799. [PubMed: 9840821]

Duda DG, Cohen KS, di Tomaso E, Au P, Klein RJ, Scadden DT, Willett CG, Jain RK. Differential CD146 expression on circulating versus tissue endothelial cells in rectal cancer patients: implications for circulating endothelial and progenitor cells as biomarkers for antiangiogenic therapy. J Clin Oncol 2006;24:1449–1453. [PubMed: 16549839]

Duda DG, Cohen KS, Au P, Scadden DT, Willett CG, Jain RK. Detection of circulating endothelial cells: CD146-based magnetic separation enrichment or flow cytometric assay? J Clin Oncol. 2007in press

Dvorak HF. Vascular permeability factor/vascular endothelial growth factor: a critical cytokine in tumor angiogenesis and a potential target for diagnosis and therapy. J Clin Oncol 2002;20:4368–4380. [PubMed: 12409337]

Fomchenko EI, Holland EC. Origins of brain tumors—a disease of stem cells? Nat Clin Pract Neurol 2006;2:288–289. [PubMed: 16932567]

Grossman SA, Batara JF. Current management of glioblastoma multiforme. Semin Oncol 2004;31:635–644. [PubMed: 15497116]

Hollander, M.; Wolfe, DA. Nonparametrical Statistical Inference. New York: John Wiley & Sons; 1973.

Ince WL, Jubb AM, Holden SN, Holmgren EB, Tobin P, Sridhar M, Hurwitz HI, Kabbinavar F, Novotny WF, Hillan KJ, Koeppen H. Association of k-ras, b-raf, and p53 status with the treatment effect of bevacizumab. J Natl Cancer Inst 2005;97:981–989. [PubMed: 15998951]

Jackson A, Jayson GC, Li KL, Zhu XP, Checkley DR, Tessier JJ, Waterton JC. Reproducibility of quantitative dynamic contrast-enhanced MRI in newly presenting glioma. Br J Radiol 2003;76:153–162. [PubMed: 12684231]

Jain RK, Safabakhsh N, Sckell A, Chen Y, Jiang P, Benjamin L, Yuan F, Keshet E. Endothelial cell death, angiogenesis, and microvascular function after castration in an androgen-dependent tumor: role of vascular endothelial growth factor. Proc Natl Acad Sci USA 1998;95:10820–10825. [PubMed: 9724788]

Jain RK. Normalizing tumor vasculature with anti-angiogenic therapy: a new paradigm for combination therapy. Nat Med 2001;7:987–989. [PubMed: 11533692]

Jain RK. Normalization of tumor vasculature: an emerging concept in antiangiogenic therapy. Science 2005;307:58–62. [PubMed: 15637262]

Jain RK, Duda DG, Clark JW, Loeffler JS. Lessons from phase III clinical trials on anti-VEGF therapy for cancer. Nat Clin Pract Oncol 2006;3:24–40. [PubMed: 16407877]

Jubb AM, Hurwitz HI, Bai W, Holmgren EB, Tobin P, Guerrero AS, Kabbinavar F, Holden SN, Novotny WF, Frantz GD, et al. Impact of vascular endothelial growth factor-A expression, thrombospondin-2 expression, and microvessel density on the treatment effect of bevacizumab in metastatic colorectal cancer. J Clin Oncol 2006;24:217–227. [PubMed: 16365183]

Kadambi A, Mouta Carreira C, Yun CO, Padera TP, Dolmans DE, Carmeliet P, Fukumura D, Jain RK. Vascular endothelial growth factor (VEGF)-C differentially affects tumor vascular function and leukocyte recruitment: role of VEGF-receptor 2 and host VEGF-A. Cancer Res 2001;61:2404–2408. [PubMed: 11289105]

Law M, Cha S, Knopp EA, Johnson G, Arnett J, Litt AW. High-grade gliomas and solitary metastases: differentiation by using perfusion and proton spectroscopic MR imaging. Radiology 2002;222:715–721. [PubMed: 11867790]

Lichy MP, Wietek BM, Mugler JP 3rd, Horger W, Menzel MI, Anastasiadis A, Siegmann K, Niemeyer T, Konigsrainer A, Kiefer B, et al. Magnetic resonance imaging of the body trunk using a single-slab, 3-dimensional, T2-weighted turbo-spin-echo sequence with high sampling efficiency (SPACE) for high spatial resolution imaging: initial clinical experiences. Invest Radiol 2005;40:754–760. [PubMed: 16304477]

Motzer RJ, Michaelson MD, Redman BG, Hudes GR, Wilding G, Figlin RA, Ginsberg MS, Kim ST, Baum CM, DePrimo SE, et al. Activity of SU11248, a multitargeted inhibitor of vascular endothelial growth factor receptor and platelet-derived growth factor receptor, in patients with metastatic renal cell carcinoma. J Clin Oncol 2006;24:16–24. [PubMed: 16330672]

Oh J, Cha S, Aiken AH, Han ET, Crane JC, Stainsby JA, Wright GA, Dillon WP, Nelson SJ. Quantitative apparent diffusion coefficients and T2 relaxation times in characterizing contrast enhancing brain tumors and regions of peritumoral edema. J Magn Reson Imaging 2005;21:701–708. [PubMed: 15906339]

Ostergaard L, Sorensen AG, Kwong KK, Weisskoff RM, Gyldensted C, Rosen BR. High resolution measurement of cerebral blood flow using intravascular tracer bolus passages. Part II: Experimental comparison and preliminary results. Magn Reson Med 1996;36:726–736. [PubMed: 8916023]

Pathak AP, Schmainda KM, Ward BD, Linderman JR, Rebro KJ, Greene AS. MR-derived cerebral blood volume maps: issues regarding histological validation and assessment of tumor angiogenesis. Magn Reson Med 2001;46:735–747. [PubMed: 11590650]

Pope WB, Lai A, Nghiemphu P, Mischel P, Cloughesy TF. MRI in patients with high-grade gliomas treated with bevacizumab and chemotherapy. Neurology 2006;66:1258–1260. [PubMed: 16636248]

Prados MD, Lamborn K, Yung WK, Jaeckle K, Robins HI, Mehta M, Fine HA, Wen PY, Cloughesy T, Chang S, et al. A phase 2 trial of irinotecan (CPT-11) in patients with recurrent malignant glioma: a North American Brain Tumor Consortium study. Neurooncol 2006;8:189–193.

Rafii S, Lyden D, Benezra R, Hattori K, Heissig B. Vascular and haematopoietic stem cells: novel targets for anti-angiogenesis therapy? Nat Rev Cancer 2002;2:826–835. [PubMed: 12415253]

Reardon DA, Quinn JA, Rich JN, Desjardins A, Vredenburgh J, Gururangan S, Sathornsumetee S, Badruddoja M, McLendon R, Provenzale J, et al. Phase I trial of irinotecan plus temozolomide in adults with recurrent malignant glioma. Cancer 2005;104:1478–1486. [PubMed: 16088964]

Rempel SA, Dudas S, Ge S, Gutierrez JA. Identification and localization of the cytokine SDF1 and its receptor, CXC chemokine receptor *4*, to regions of necrosis and angiogenesis in human glioblastoma. Clin Cancer Res 2000;6:102–111. [PubMed: 10656438]

Schmainda KM, Rand SD, Joseph AM, Lund R, Ward BD, Pathak AP, Ulmer JL, Badruddoja MA, Krouwer HG. Characterization of a first-pass gradient-echo spin-echo method to predict brain tumor grade and angiogenesis. AJNR Am J Neuroradiol 2004;25:1524–1532. [PubMed: 15502131]

Segers J, Fazio VD, Ansiaux R, Martinive P, Feron O, Wallemacq P, Gallez B. Potentiation of cyclophosphamide chemotherapy using the anti-angiogenic drug thalidomide: importance of optimal scheduling to exploit the ‘normalization’ window of the tumor vasculature. Cancer Lett 2006;244:129–135.10.1016/j.canlet.2005.12.017 [PubMed: 16426744]Published online January 17, 2006

Senger DR, Galli SJ, Dvorak AM, Perruzzi CA, Harvey VS, Dvorak HF. Tumor cells secrete a vascular permeability factor that promotes accumulation of ascites fluid. Science 1983;219:983–985. [PubMed: 6823562]

Sorensen AG, Patel S, Harmath C, Bridges S, Synnott J, Sievers A, Yoon YH, Lee EJ, Yang MC, Lewis RF, et al. Comparison of diameter and perimeter methods for tumor volume calculation. J Clin Oncol 2001;19:551–557. [PubMed: 11208850]

Stoll BR, Migliorini C, Kadambi A, Munn LL, Jain RK. A mathematical model of the contribution of endothelial progenitor cells to angiogenesis in tumors: implications for antiangiogenic therapy. Blood 2003;102:2555–2561. [PubMed: 12775571]

Tofts PS, Brix G, Buckley DL, Evelhoch JL, Henderson E, Knopp MV, Larsson HB, Lee TY, Mayr NA, Parker GJ, et al. Estimating kinetic parameters from dynamic contrast-enhanced T(1)-weighted MRI of a diffusable tracer: standardized quantities and symbols. J Magn Reson Imaging 1999;10:223–232. [PubMed: 10508281]

Tong RT, Boucher Y, Kozin SV, Winkler F, Hicklin DJ, Jain RK. Vascular normalization by vascular endothelial growth factor receptor 2 blockade induces a pressure gradient across the vasculature and improves drug penetration in tumors. Cancer Res 2004;64:3731–3736. [PubMed: 15172975]

Tremont-Lukats IW, Gilbert MR. Advances in molecular therapies in patients with brain tumors. Cancer Control 2003;10:125–137. [PubMed: 12712007]

van der Kouwe AJ, Benner T, Fischl B, Schmitt F, Salat DH, Harder M, Sorensen AG, Dale AM. On-line automatic slice positioning for brain MR imaging. Neuroimage 2005;27:222–230. [PubMed: 15886023]

Wedge SR, Kendrew J, Hennequin LF, Valentine PJ, Barry ST, Brave SR, Smith NR, James NH, Dukes M, Curwen JO, et al. AZD2171: a highly potent, orally bioavailable, vascular endothelial growth factor receptor-2 tyrosine kinase inhibitor for the treatment of cancer. Cancer Res 2005;65:4389–4400. [PubMed: 15899831]

Weis SM, Cheresh DA. Pathophysiological consequences of VEGF-induced vascular permeability. Nature 2005;437:497–504. [PubMed: 16177780]

Willett CG, Boucher Y, di Tomaso E, Duda DG, Munn LL, Tong RT, Chung DC, Sahani DV, Kalva SP, Kozin SV, et al. Direct evidence that the VEGF-specific antibody bevacizumab has antivascular effects in human rectal cancer. Nat Med 2004;10:145–147. [PubMed: 14745444]

Willett CG, Boucher Y, Duda DG, di Tomaso E, Munn LL, Tong RT, Kozin SV, Petit L, Jain RK, Chung DC, et al. Surrogate markers for antiangiogenic therapy and dose-limiting toxicities for bevacizumab with radiation and chemotherapy: continued experience of a phase I trial in rectal cancer patients. J Clin Oncol 2005;23:8136–8139. [PubMed: 16258121]

Winkler F, Kozin SV, Tong R, Chae S, Booth MF, Garkavtsev I, Xu L, Hicklin DJ, Fukumura D, di Tomaso E, et al. Kinetics of vascular normalization by VEGFR2 blockade governs brain tumor response to radiation: Role of oxygenation, angiopoietin-1 and matrix metalloproteinases. Cancer Cell 2004;6:553–563. [PubMed: 15607960]

Wong ET, Hess KR, Gleason MJ, Jaeckle KA, Kyritsis AP, Prados MD, Levin VA, Yung WK. Outcomes and prognostic factors in recurrent glioma patients enrolled onto phase II clinical trials. J Clin Oncol 1999;17:2572–2578. [PubMed: 10561324]

Yoshiji H, Harris SR, Thorgeirsson UP. Vascular endothelial growth factor is essential for initial but not continued in vivo growth of human breast carcinoma cells. Cancer Res 1997;57:3924–3928. [PubMed: 9307273]

Yuan F, Chen Y, Dellian M, Safabakhsh N, Ferrara N, Jain RK. Time-dependent vascular regression and permeability changes in established human tumor xenografts induced by an anti-vascular endothelial growth factor/vascular permeability factor antibody. Proc Natl Acad Sci USA 1996;93:14765–14770. [PubMed: 8962129]

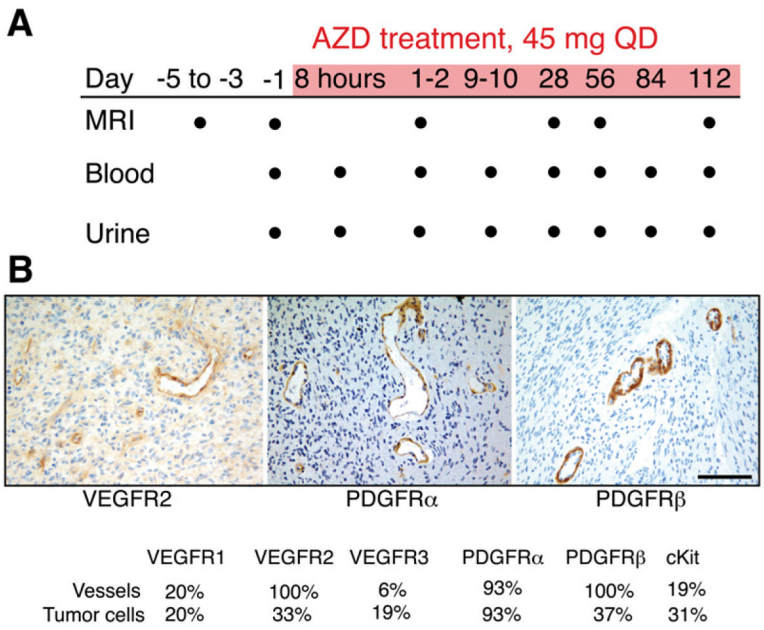


**Figure 1. Design of Clinical Trial and Target Validation by Immunohistochemistry**

(A) Trial schema. Dots indicate time points of data collection. AZD2171 was administered during the period shaded red.

(B) Representative immunohistochemistry of glioblastoma endothelium. As expected, VEGFR2 and PDGFRα are expressed in the endothelial cells. Interestingly, PDGFRβ is also highly expressed in endothelial cells. (Bar represents 100 μm for all images.)

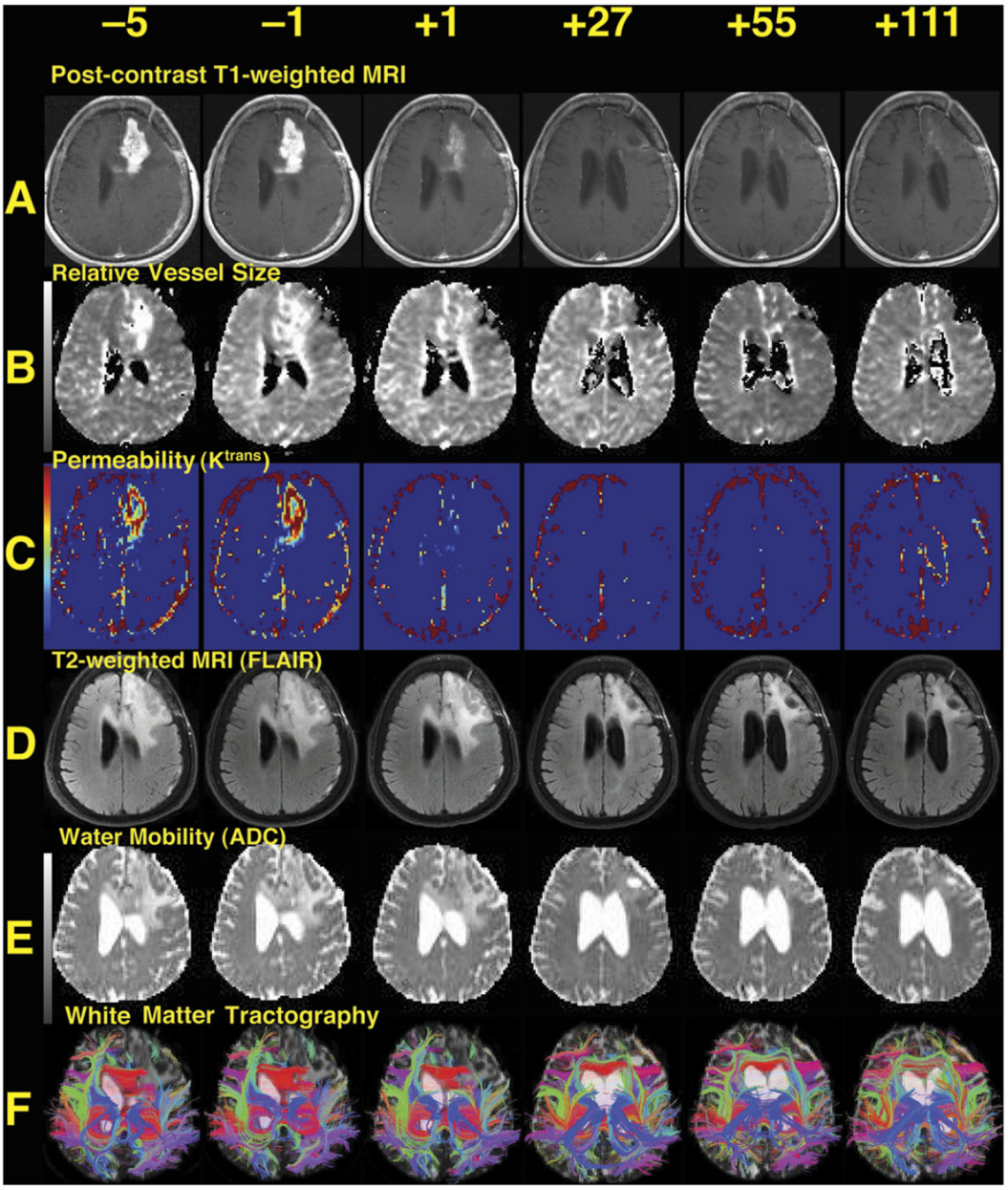


**Figure 2. Representative Images from the Best-Responding Patient, Patient 9**

(A) T1-weighted anatomic images after intravenous administration of a contrast agent (gadolinium-DTPA), demonstrating a region of bright signal corresponding to the recurrent brain tumor in the left frontal lobe shrinking over time (all images are displayed per standard radiographic convention). Note also the decreased mass effect on the left lateral ventricle.

(B) Map of relative microvessel size, also showing decrease over time.

(C) Maps of $K^{trans}$, a measure of blood-brain barrier permeability. Note the substantial change after the first dose.

(D) T2-weighted images acquired with a fluid-attenuated inversion recovery sequence (FLAIR), where edema is seen surrounding the tumor enhancement evident in (A), also decreasing over time.

(E) Images of apparent diffusion coefficient (ADC) demonstrating water mobility, which identifies areas of vasogenic edema as high (bright) signal surrounding the region of enhancing tumor; these also reduce over time. The displacement of the ventricle is also reduced over time. (F) Tractography. These images demonstrate directional water mobility suggesting the presence of white matter tracts. As the vasogenic edema decreases and the mass effect subsides, these white matter tracts become more evident. A movie of day −1 and day 28 time points is available in the Supplemental Data (Movie S1).

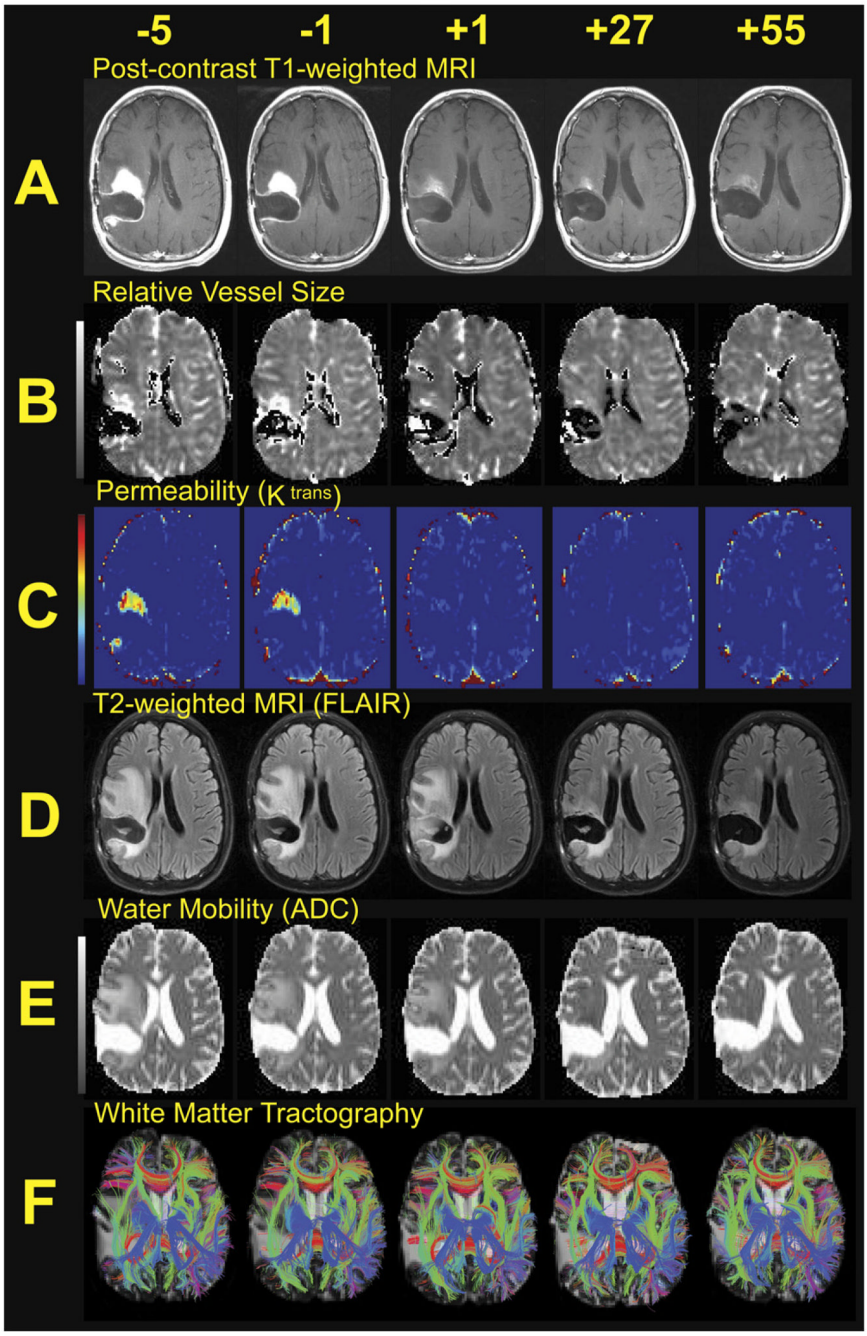


**Figure 3. Representative Images from a Moderately Responding Patient**

(A–F) The types of images are the same as in Figure 2. Typical of most patients, there was substantial and prolonged reduction of enhancement and peritumoral edema, with some rebound of vessel size at day 55.

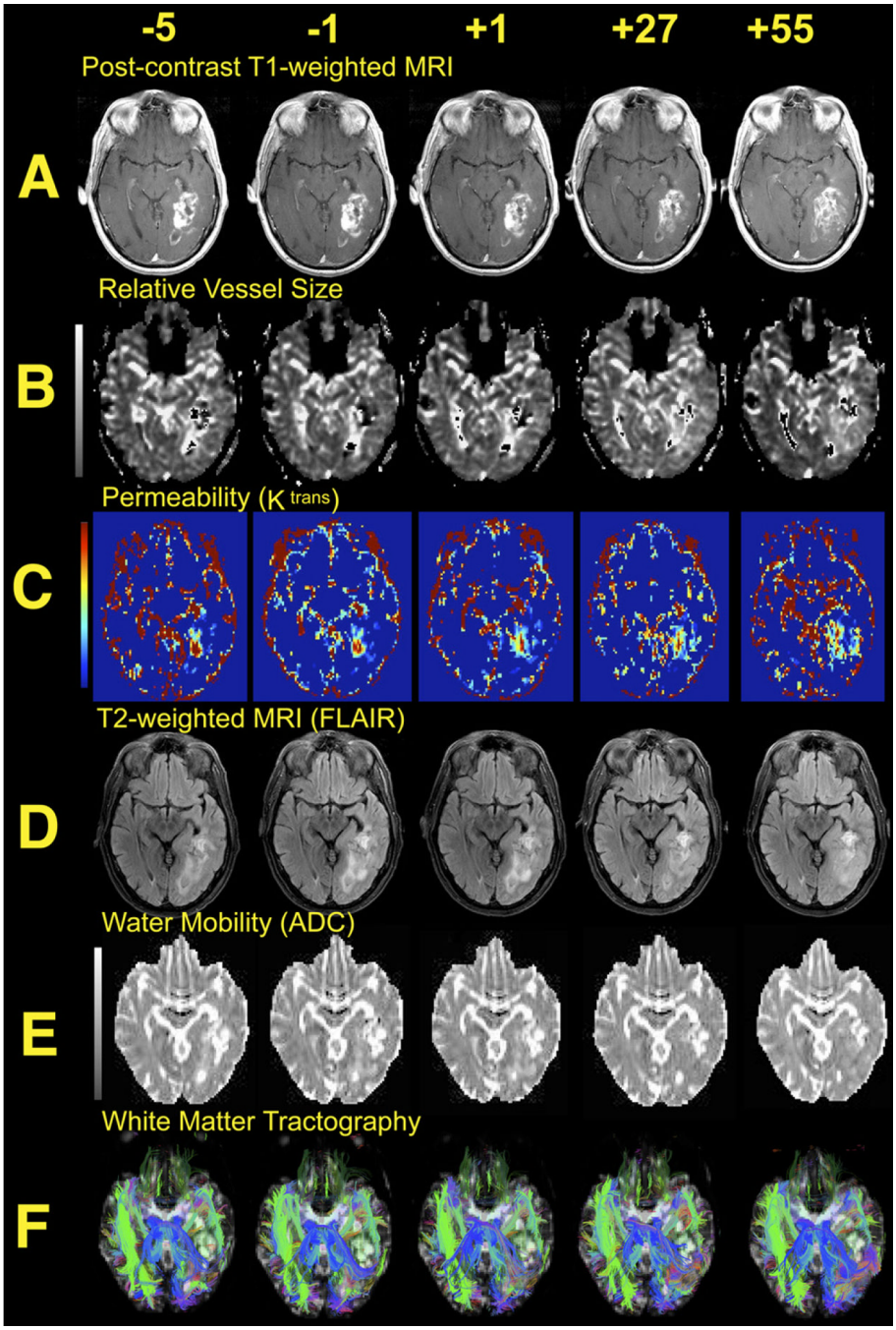


**Figure 4. Representative Images from the Worst-Responding Patient**

(A–F) The types of images are the same as in Figure 2. This patient had no substantial reduction in permeability, mass effect, or vessel size. A slight decrease in edema is evident on the FLAIR and ADC images at day 27, but this reverts by day 55.

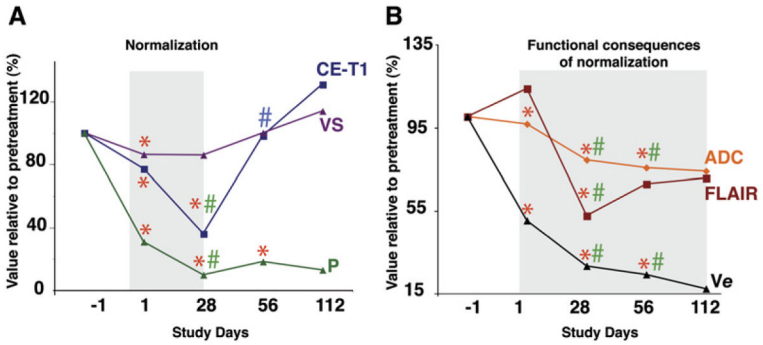


**Figure 5. Changes in Imaging Parameters over Time**

(A) Median values for contrast-enhanced T1-weighted tumor volume (CE-T1), vessel size (VS), and permeability (P) of the tumor over time as measured by an independent expert. Day −1 was set as 100% in all lesions, and changes during AZD2171 treatment were plotted for all 16 patients. Note the rebound of CE-T1 volume and vessel size after day 28, which indicates a partial closure of the normalization window.

(B) Median values of T2-weighted abnormality volume measured in fluid-attenuated inversion recovery images (FLAIR), apparent diffusion coefficient (ADC), and extracellular-extravascular volume fraction ($v_e$) prior to and during treatment showing a sustained decrease of edema while taking AZD2171. (*$p < 0.05$ for values compared with day −1; $^{\#}p < 0.05$ for values compared with day +1. For full measurement details see Table S3.)

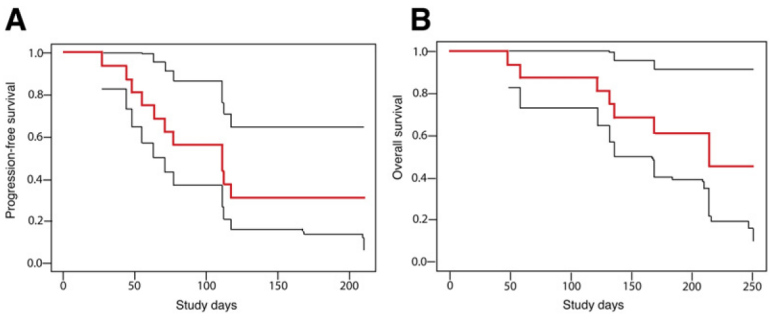


**Figure 6. Kaplan-Meier Survival Distributions**

(A) Progression-free survival and (B) overall survival in sixteen recurrent glioblastoma patients receiving AZD2171 (bold red lines) accompanied by upper and lower 95% confidence limits (thin black lines).

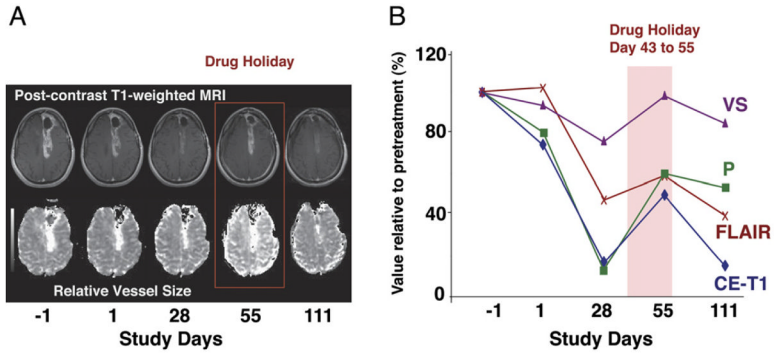


**Figure 7. Reversibility of Normalization**

(A) Vascular and volume changes as a function of time in a patient who did not take drug from days 43 through 56 and was imaged on day 55 (shown as drug holiday). T1-weighted anatomic images after intravenous administration of gadolinium-DTPA, similar to Figure 2. Note that at day 55 there is a rebound in tumor enhancement, which decreases again after restarting the drug as seen on follow-up imaging on day 110. In this patient, maps of relative vessel size (similar to Figure 1C) also show fluctuation with the drug holiday and resumption of AZD2171 treatment.

(B) Measurements of imaging parameters confirm the reversibility of vascular normalization by drug interruption followed by renormalization after AZD2171 is resumed.

**Table 1**

Blood Biomarker Analyses in Relation to Radiographic Tumor Response, Drug Holidays, and Vessel Size

| | **Effect of Tumor Progression** | **Effect of Drug Holidays** | **Effect on Vessel Size** |
|---|---|---|---|
| VEGF | −15% | ***−43%*** | 0.111 |
| | [−32% to +7%] | ***[−58%*** to ***−22%]*** | [−0.159 to 0.381] |
| | p = 0.1701 | ***p = 0.0005*** | p = 0.4151 |
| PlGF | ***−32%*** | ***−58%*** | 0.023 |
| | ***[−49%*** to ***−9%]*** | ***[−72%*** to ***−38%]*** | [−0.180 to 0.225] |
| | ***p = 0.0094*** | ***p < 0.0001*** | p = 0.8224 |
| sVEGFR1 | +5% | +10% | −0.137 |
| | [−8% to +21%] | [−8% to +31%] | [−0.593 to 0.319] |
| | p = 0.4775 | p = 0.2963 | p = 0.5515 |
| sVEGFR2 | ***+13%*** | +11% | −0.002 |
| | ***[0%*** to ***+26%]*** | [−6% to +30%] | [−0.553 to 0. 549] |
| | ***p = 0.0420*** | p = 0.2115 | p = 0.8224 |
| bFGF | ***+59%*** | +92% | ***0.138*** |
| | ***[+2%*** to ***+148%]*** | [−3% to +280%] | ***[0.008*** to ***0.268]*** |
| | ***p = 0.0417*** | p = 0.0606 | ***p = 0.0372*** |
| SDF1α | ***+12%*** | +4% | ***0.667*** |
| | ***[+2%*** to ***+22%]*** | [−7% to +18%] | ***[0.075*** to ***1.258]*** |
| | ***p = 0.0158*** | p = 0.4794 | ***p = 0.0227*** |
| Viable CECs | ***+53%*** | +11% | 0.147 |
| | ***[+3%*** to ***+128%]*** | [−38% to +96%] | [−0.026 to 0.320] |
| | ***p = 0.0347*** | p = 0.7283 | p = 0.0945 |
| CPCs | −3% | ***+75%*** | 0.130 |
| | [−29% to +34%] | ***[+15%*** to ***+167%]*** | [−0.103 to 0.364] |
| | p = 0.8741 | ***p = 0.0097*** | p = 0.2683 |

Estimates are determined as described in Experimental Procedures and represent the percent change in plasma concentration (for cytokines) or in circulating cells (CECs and CPCs) associated with a doubling in tumor volume assessed by CE-T1 imaging (left column) or drug holiday (middle column); estimates in the right column represent mean absolute change in vessel size associated with a doubling of the tested biomarker variable, after adjusting for time trend and initial vessel size. Square brackets present 95% confidence intervals for the point estimates. Significant correlations are depicted in bold and italics.